

# INFLUENCE OF HIGH VOLTAGE WAVEFORM AND FREQUENCY ON THE ELIMINATION OF ELECTRIC CHARGES AT THE SURFACE OF POLYPROPYLENE FILMS

AKILA MESSAOUDENE<sup>1</sup>, LUCIAN DASCALESCU<sup>2</sup>, BOUKHALFA BENDAHMANE<sup>1</sup>

**Keywords:** Ac corona discharge; Polypropylene films; Electrostatic charge elimination; Surface electric potential.

One of the primary sources of fires and explosions in manufacturing processes is the build-up of electric charge during the manipulation of insulating materials. The challenge is to find an appropriate method to eliminate these charges. This present work aims to evaluate the influence of the frequency and the waveform of the high voltage on the efficiency of charge neutralization of electrically charged polypropylene films using a triode-type corona electrode configuration. A positive polarity DC high-voltage power supply was employed for the corona charging of the samples, which were then neutralized using the triode-type electrode system energized from a sinusoidal-, a triangular- or a square-wave AC high-voltage supply. The electric charge state of the PP film was characterized by means of a non-contact electrostatic voltmeter for measuring the electric potential along the central axis of the sample. The neutralization rate increased with the frequency for both sinusoidal and triangular AC high voltages. At all frequencies, the square-wave high-voltage was more efficient than the others. At 50 Hz, the surface charge was eliminated after several successive exposures of the samples to the discharge generated from the triode-type corona electrode connected to a sinusoidal HV supply.

## 1. INTRODUCTION

The generation and accumulation of electric charges on the surface of insulating materials by triboelectric effect is one of the major sources of electrostatic hazards in industry [1,2]. The prevention of electrostatic discharges is a key issue especially for processes that use flammable solvents or involve the fabrication of electronic components [3].

Eliminating the electrical charges at the surface of an insulating body can be achieved by using either passive or active static dissipaters [4]. The former typically consist in a row of needles connected to the ground, so that an electric field occurs in the space between them and the charged surface. The electric field is much more intense near the sharp tips of the needles and generate a corona discharge that forms negative ions if the surface of the insulator is charged positively. The negative ions are driven by the electrical field forces to the positively charged surface and start neutralizing the existing charges. The process stops when the charge density at the surface of the insulator decreased to a level that is not enough for maintaining the electric field intensity required for sustaining the corona discharge. Therefore, the passive dissipaters cannot eliminate the charge at the surface of insulators.

The simplest active dissipator also consists in a row of needles, but which are energized from an AC high-voltage supply [5]. Positive and negative ions are alternately produced by corona discharge at the needle tips. Whatever the sign of the charge on the insulating body, the oppositely charged ion will eliminate it. However, if uncontrolled, this active neutralization may cause the reversal of the polarity of the surface. In several previous papers on the active neutralization, the authors evaluated the effects of the various factors the efficiency of the process, including waveform and frequency of the high-voltage, as well as the configuration of the electrode system and nature of the treated materials [6–11].

Corona discharge has been extensively studied in relation with applications to electrostatic precipitation of dust [12] and electrostatic separation of granular materials [13]. The active neutralization using a triode-type electrode system was found to be a simple and efficient process. By grounding the grid of triode type electrode, a zero potential could be imposed on the charged surface. It is thus possible to better control the neutralization process [14–16]. The experimental studies pointed out that the active neutralization depends on the amplitude of the sinusoidal high voltage applied to the corona electrode, the duration of exposure to the discharge, the scanning speed and the spacing between the neutralizer and the substrate [17,18].

This paper aims to evaluate the efficiency of polypropylene films neutralization using an AC corona generated by a triode-type configuration energized from either a sinusoidal-, a triangular- or a square-wave high-voltage supply of various frequencies. The experiments were performed on positive corona charged films. The electric potential profiles at the surface of the films before and after neutralization were obtained by using a non-contact electrostatic voltmeter and enabled the calculation of a charge neutralization rate.

## 2. MATERIALS AND METHODS

Figure 1 shows that the experimental apparatus has two sections, one for charging and the other for charge elimination. The electric charging section consists of a triode-type electrode [17,19] composed of a high-voltage wire-type dual electrode [13] and a grid electrode, the latter being connected to ground through a resistor  $R_g = 100 \text{ M}\Omega$ . The dual electrode consists of a tungsten wire (diameter: 0.2 mm) suspended by a metallic cylinder (diameter: 26 mm) at 34 mm from the axis. The assembly wire and cylinder are energized from an adjustable DC high-voltage supply, 100 kV, 3 mA (positive polarity).

<sup>1</sup> Laboratoire de Génie Electrique de Bejaia, Faculté de Technologie, Université de Bejaia (06000), Algérie

<sup>2</sup> PPRIME Institute, UPR 3346 CNRS – University of Poitiers – ENSMA, IUT Angoulême, France

Corresponding author: akila.messaoudene@univ-bejaia.dz

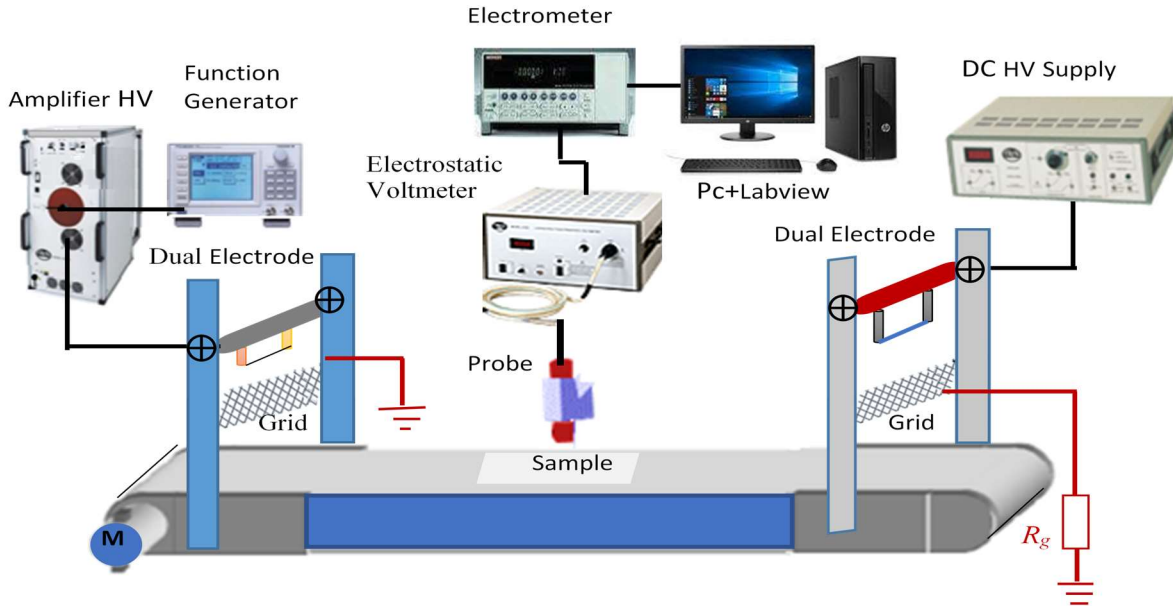


Fig. 1 – Experimental set-up for the measurement of the surface potential after charging and after discharging the PP films.

The distance between the wire and the surface of the plate electrode is 30 mm and the metallic grid is placed at equal distance (15 mm) from both. By adjusting the resistor  $R_g$ , a potential  $V_g = R_g \times I_g$  is imposed between the grid and the grounded plate electrode. Thus, the charging of the sample is completed when the potential at the surface of the sample is equal to that of the grid (the electric field between the grid and the surface of the sample is nil).

The repartition of the surface potential along the central axis of the sample is measured with an electrostatic voltmeter (model 341B), equipped with an electrostatic probe (model 3450, Trek, Inc., Medina, NY), and recorded via an electrometer (model 6514, Keithley Instruments, Cleveland, OH), which is connected to a computer. The acquisition and processing of experimental data are performed using a virtual instrument (LabView).

The charge elimination section consists of another triode-type electrode system like the one described earlier. The corona electrode is connected to a high-voltage amplifier 30 kV, 20 mA (model 30/20 A, Trek Inc., Medina, NY) and the grid is directly connected to the ground. The maximum value of the alternating high-voltage  $U_n$  and the frequency are adjusted using a synthesized function generator (model FG300, Yokogawa, Japan). The sample is neutralized by passing it at constant speed through the charge elimination section.

In all the experiments described in this paper, the samples consisted of polypropylene (PP) films with dimensions: 110 mm x 100 mm x 40  $\mu$ m and were maintained for 10 s in the corona discharge generated by the triode-type electrode system. The transversal central axis of the samples was in the vertical plane defined by the axes of the wire and the cylinder of the dual-type corona electrode. A conveyor belt supported the sample and, when the 10 s charging was completed, transferred it to the surface potential measurement and the charge elimination sections of the experimental set-up, at a speed  $v_b = 3$  cm/s.

With the sample moving at this speed, the electric potential was measured in 20 points at its surface. The high-

voltage amplifier that energizes the triode-type neutralization electrode system was turned on only for 4 s, the time needed for the sample to be conveyed through the charge elimination section. As soon as the sample exited the active neutralization zone, the conveyor belt transferred it back to the electric potential measurement section. In this way, the electric potential profile at the surface of the sample was measured also after the charge elimination.

The efficiency of charge elimination was evaluated by calculating the neutralization rate  $N$ , expressed as a function of the maximum surface potential before ( $V_1$ ) and after ( $V_2$ ) the exposure of the sample to the action of the AC corona discharge [17]:

$$N[\%] = \left(1 - \frac{V_2}{V_1}\right) \cdot 100. \quad (1)$$

The experiments were performed in ambient air (temperature: 23 – 25 °C; relative humidity: 59 % – 64 %).

### 3. RESULTS AND DISCUSSION

The potential profiles measured before and after neutralization are presented as a function of the position  $x$  along the longitudinal axis of the sample. The position  $x = 0$  corresponds to the median transversal axis of the sample.

#### 3.1. FREQUENCY EFFECT ON THE NEUTRALIZATION EFFICIENCY

Figures 2 and 3 show the distribution of surface potential after charging the PP samples with a grid voltage  $V_g = 2.5$  kV and after discharging them with a corona electrode energized from a generator of sinusoidal and triangular AC voltages of the same amplitude  $U_n = 13$  kV, for various frequencies  $f = 100$  Hz, 200 Hz, 300 Hz and 400 Hz.

The charging profiles were highly reproducible. Therefore, only one such profile is represented on the figures. These profiles show that – unsurprisingly – the maximum potential was obtained at the sample center, located just below the active electrode, and subjected of the

most intense flux of monopolar ions.

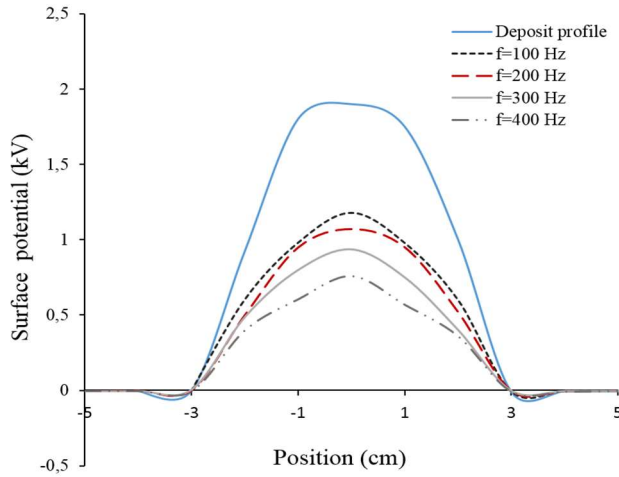


Fig. 2 – Neutralization of PP samples corona-charged at  $V_g = 2.5$  kV by passing them under the triode-type corona electrode system energized by sinusoidal-wave high-voltage of amplitude  $U_n = 13$  kV and various frequencies.

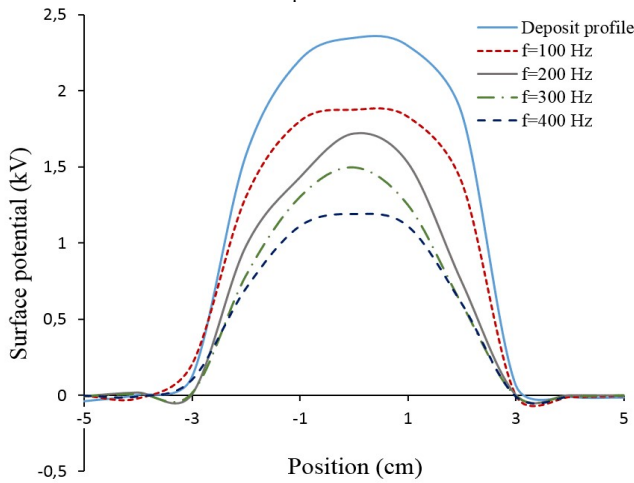


Fig.3 – Neutralization of PP samples corona-charged at  $V_g = 2.5$  kV by passing them under the triode-type corona electrode system energized by sinusoidal-wave high-voltage of amplitude  $U_n = 13$  kV and various frequencies.

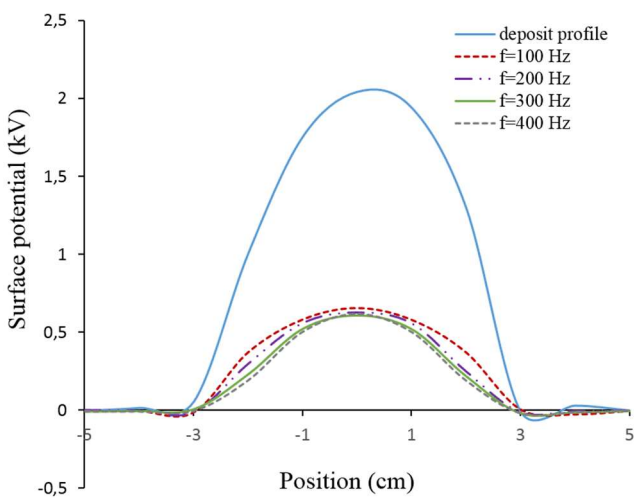


Fig. 4 – Neutralization of PP samples corona-charged at  $V_g = 2.5$  kV by passing them under the triode-type corona electrode system energized by square-wave high-voltage of amplitude  $U_n = 13$  kV and various frequencies.

The shape of the neutralization profiles obtained at a given frequency of the AC high-voltage supply was also highly reproducible and like that of the charging profiles. This

means that the neutralization rate is not significantly affected by the charge level at the surface of the sample before being exposed to the AC corona discharge. However, the efficiency of the neutralization depends on the wave-shape of the applied AC high-voltage and significantly increases with the frequency of the AC signal. This can be explained by the kinetics of the bipolar ions alternatively emitted by the triode-type corona electrode. Thus, for a similar exposure duration to the AC corona discharge (same speed of the conveyor belt), the neutralization is faster for the sinusoidal wave-shape energization of the triode-type electrode system, as the energy transferred in the discharge is higher than for the triangular wave-shape.

In the case of the square-wave AC high voltage (Fig. 4), the outcome of the neutralization depended to a much lesser extent on the frequency. The residual potential recorded at the center was close to 0.5 kV for all frequencies, as the applied voltage was beyond the corona-inception threshold during the entire cycle (both negative and positive half cycles), and bi-polar ions were generated in a larger quantity, and this independently of the frequency.

### 3.2. WAVEFORM EFFECT ON THE NEUTRALIZATION EFFECIENCY

Fig. 5 illustrates the neutralization rate as a function of the frequency for different wave-shapes of the AC high-voltage that energizes the electrode system. The best neutralization rates (roughly 70 %) were recorded for the case of a square-wave energization. In the condition of these particular experiments, the sinusoidal-wave and triangular-wave high voltages eliminate less than 55 % and 35 % of the charges, even in the most favorable case, i.e. when using a frequency of 400 Hz.

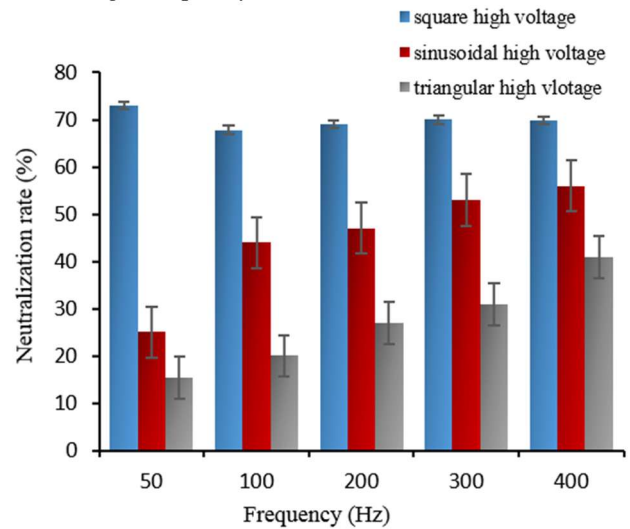


Fig. 5– Neutralization rate of PP samples corona-charged at  $V_g = 2.5$  kV, as function a frequency, for various waveforms of the high-voltage applied to the triode-type electrode system.

The surface potential profiles of Fig. 6 are associated to 3 sets of samples charged with an intensity  $I_g = 25$   $\mu$ A ( $V_g = 2.5$  kV) and exposed to the neutralization AC corona discharge using high voltages of different waveforms, of amplitude  $U_n = 13$  kV, at frequency  $f = 50$  Hz. As expected, the neutralization was more effective for square and sinusoidal high voltages. The maximum residual potential was roughly 500 V ( $N \approx 75$  %), in the case of square-wave high voltage, and slightly higher than 1 kV ( $N \approx 50$  %), when using the sinusoidal-wave neutralization.

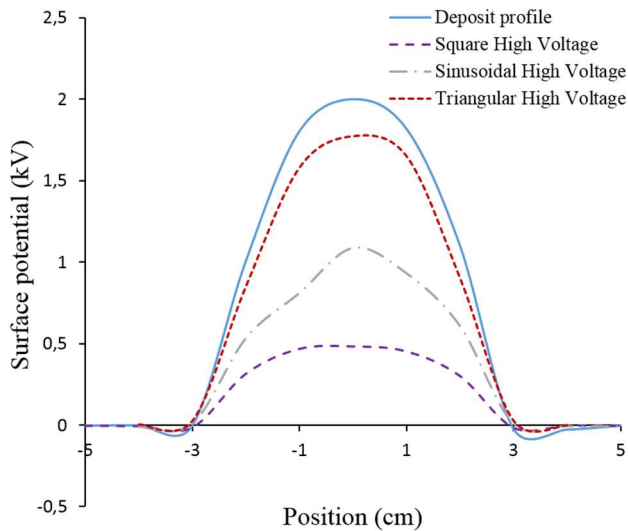


Fig.6 – Effect of waveform of the high voltage on the neutralization efficiency, at  $f= 50$  Hz. The PP sample was corona-charged at  $V_g= 2.5$  kV.

The lowest efficiency was recorded in the case when the triode-type corona electrode system was supplied with a triangular-wave high voltage. As a matter of fact, the neutralization requires high energy, to generate the bi-polar ions and their drift to the charged sample.

During the neutralization process, this energy is harnessed to reach the surface of the sample and reach the trapped charges in bulk [18]. The energy of the corona discharge depends on the amplitude of the neutralization voltage. Therefore, it is expected that better neutralization could be obtained at higher amplitudes of the high voltage applied to the electrode system.

### 3.3. SUCCESSIVE NEUTRALIZATIONS AS BEST SOLUTION

Figure 7 presents the profiles obtained after three successive neutralizations, applied to the same sample charged with  $V_g = 3$  kV.

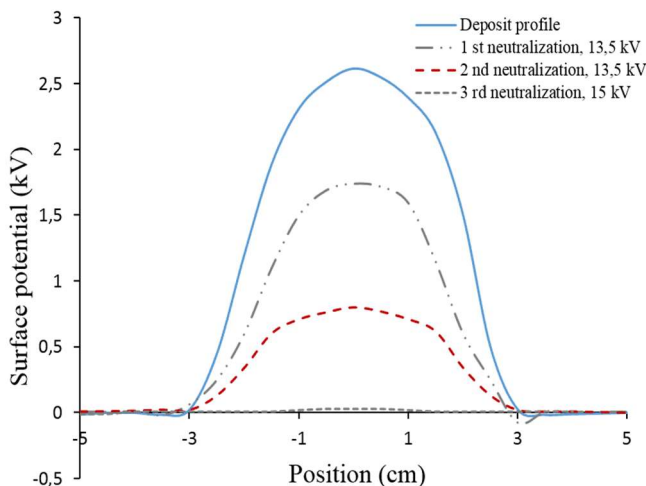


Fig.7 – Effect of successive neutralizations on the neutralization efficiency.

The neutralization test was carried out based on the sinusoidal voltage with frequency 50 Hz. The first and the second neutralization are performed with the amplitude voltage  $U_n= 13,5$  kV followed with the third neutralization of the amplitude  $U_n= 15$  kV. After the first passage, the neutralization rate is equal to 33, 3%. The second passage

corresponding to a neutralization rate of 70 % leads to better elimination of residual charges. After the third passage, the neutrality of all the points of the sample is obtained.

## 4. CONCLUSIONS

The results obtained during the experiments described in the paper lead to the following conclusions:

- 1) The waveform of the AC high voltage applied to the neutralizer has a remarkable effect on the efficiency of the process.
- 2) At similar amplitude and frequency, the sinusoidal-wave high voltage ensures a better elimination of the static charge than the triangular-wave. On the other hand, the square-wave neutralization is more efficient than the sinusoidal and the triangular ones.
- 3) The sinusoidal- and square-wave neutralizations require lower amplitudes, for the same effect.
- 4) At higher frequency, the surface and volume residual charges are more likely to be eliminated.
- 5) The square-wave neutralization only marginally depends on the frequency of the AC high voltage.
- 6) For a well-defined frequency range, the efficiency of sinusoidal- and triangular-wave neutralizations is proportional to the frequency of the applied high voltage.
- 7) To improve the controlled neutralization efficiency, the solution is to employ successive neutralizations.

## ACKNOWLEDGMENT

This research work is carried out under the patronage of the General Directorate of Algerian Scientific Research and Technological Development DGRSDT.

Received on November 4, 2021

## REFERENCES

1. S. H. Voldman, *The state of the art of electrostatic discharge protection physics technology, circuits, design, simulation, and scaling*, IEEE J. Solid-state Circuits., **34**, pp. 1272-1282, 1999.
2. C. Duvvury, E. A. Amerasekera, *ESD in silicon integrated circuits*, USA, John Wiley, 2002.
3. K. Robinson, W. Durkink, *Electrostatic issues in roll-to-roll manufacturing operation*, IEEE Trans. Ind. Appl., **46**, 6, pp. 2172-2178, 2010.
4. K. Robinson, *Assessing passive static dissipators*. Proc. 2016 Electrostatics Joint Conference, Purdue University, West Lafayette, IN June 13-16, 2016.
5. A. Ohsawa, *Efficient charge neutralization with an AC corona ionizer*. J. Electrostat., **65**, pp. 598-606, 2007.
6. B. Yahiaoui, B. Tabti, M. Megherbi, A. Antoniu, M. C. Ploeanu, L. Dascalescu, *AC corona neutralization of positively and negatively charged polypropylene non-woven fabrics*, IEEE Trans. Ind. Appl., **20**, pp. 1516-1522, 2013.
7. B. Yahiaoui, M. Megherbi, A. Smaili, B. Tabti, A. Antoniu, L. Dascalescu, *Distribution of electric potential at the surface of corona charged polypropylene non-woven fabrics after neutralization*, IEEE Trans. Ind. Appl., **49**, 1, pp. 1758-1766, 2013.
8. B. Yahiaoui, M. Megherbi, B. Tabti, L. Dascalescu, *Sinusoidal, triangular or square alternating voltages neutralization of electrostatics charges on the surface of polypropylene nonwoven fabric*, IEEE Trans. Ind. Appl., **51**, pp. 685-691, 2015.
9. A. Antoniu, A. Smaili, I.V. Vacar. M. C. Ploeanu, L. Dascalescu, *Sinusoidal and triangular AC high-voltage neutralizers for accelerated discharge of non-woven fibrous dielectrics*, IEEE Trans. Ind. Appl., **48**, pp. 857-863, 2012.
10. A. Antoniu, B. Tabti, M. C. Ploeanu, L. Dascalescu, *Accelerated discharge of corona-charged non-woven fabrics*, IEEE Trans. Ind. Appl., **46**, pp. 1188-1193, 2010.
11. M. Kachi, L. Dascalescu, L. Herous, M. Nemamcha, *Experimental study*

- of charge neutralization at the surface of Granular layers of insulating material*, IEEE Trans. Ind. Appl., **48**, pp. 691-698, 2013.
12. F. Miloua, A. Tilmatine, L. Dascalescu, *Optimization of filtration efficiency of a wire-cylinder electrostatic precipitator*, Rev. Roum. Sci. Techn- Électrotechn. et Énerg., **58**, 2, pp. 153-162, 2013.
13. LM. Dumitran, LV Badicu, MC Ploeanu, L. Dascalescu, *Efficiency of dual wire-cylinder electrodes used in electrostatic separators*, Rev. Roum. Sci. Techn- Électrotechn. et Énerg., **55**, 2, pp. 171-180, 2010.
14. A. Messaoudène, M.R.Mekidèche, B.Bendahmane, B. Tabti, L. Dascalescu, *Caractérisation Expérimentale de la neutralisation active et contrôlée des films en polypropylène*, 11<sup>ème</sup> Conférence de la Société Française d'Électrostatique : SFE 2018, Grenoble (France), 29-31 Aout, 2018.
15. A. Messaoudène, M.R.Mekidèche, B.Bendahmane, B. Tabti, K. Medles, L. Dascalescu, *Experimental modeling and optimization of the active neutralization of a PP film, using design of experiments methodology*, IEEE/IAS Ann. Meet., Baltimore, MD, 30 Sept–10 Oct, 2019.
16. B. Bendahmane, A. Messaoudène, L. Dascalescu, *Alternating Current Corona of Charged Filters Media*, IEEE 3<sup>rd</sup> International Conference on Dielectrics, Valencia (Spain), 5-31 July 2020.
17. A. Messaoudène, M.R.Mekidèche, B.Bendahmane, B. Tabti, K. Medles, L. Dascalescu, *Optimization of the active neutralization of polypropylene films using response surface methodology*, IEEE Trans. Ind. Appl., **56**, 5, pp. 5463-5471, 2020.
18. A. Messaoudène, M.R.Mekidèche, B. Bendahmane, B. Tabti, L. Dascalescu, *Experimental study of controlled active neutralization of polypropylene films*, J. Electrostat, **103**, 103400, 2020.
19. K. Rouagdia, L.Dascalescu, *Robust optimum operating conditions for AC corona neutralization of insulating materials*, Rev. Roum. Sci. Techn. – Électrotechn. Et Énerg., **65**, 1-2, pp. 5-10, 2020.